Journal of Wasit for Science and Medicine 2025: 18, (4), 101-114

Development of Nanostructured CuO Films Using DC Magnetron Sputtering for Ammonia Gas Sensing Applications

Basima Saleem Dawood

Department of Physics, College of Science, University of Wasit, Iraq.

Abstract

In this study, nanostructured copper oxide (CuO) thin films were prepared using DC magnetron sputtering for application as an ammonia (NH_3) gas sensor. The films were deposited on glass substrates under different Ar:O_2 gas ratios (1:1 and 2:1), and the effect of post-deposition thermal treatment on structural and morphological properties was investigated. XRD analysis revealed that the films were polycrystalline with a clear preferred orientation, while FE-SEM images showed uniform nanosized grains with average sizes ranging from 35 to 44 nm, depending on the gas mixture ratio, indicating controlled crystal growth. FT-IR spectroscopy confirmed the presence of chemical bonds characteristic of copper oxide, verifying the formation of the desired. Gas sensing tests demonstrated effective NH_3 detection, with sensitivity directly influenced by grain size, surface roughness, and surface area, which facilitated efficient gas adsorption and rapid response and recovery these results indicate that DC magnetron sputtered nanostructured CuO films are promising candidates for high-performance ammonia gas sensors. Furthermore, sensor performance can be optimized by carefully controlling gas ratios and thermal treatment conditions, providing potential for practical applications in industrial and environmental NH_3 monitoring.

Keywords: Copper Oxide (CuO), Nanostructured Thin Films, and Gas sensing.

1. Introduction

The current era is marked by the dominance of modern sciences across all aspects of life, particularly in technological and industrial fields. Rapid advancements in scientific research have led to the development of new materials and techniques, among which semiconductors play a crucial role in precise electronic devices. Semiconductors are materials which electrical conductivity between conductors and insulators, and the study of thin films

made from them is essential for advancing electronic and optical applications, such as sensors, solar cells, and gas detection devices [1]. Recently, gas sensing, as a typical application in smart systems, has received increasing attention in both industry and academia. Gas sensing technology has become increasingly important due to its widespread applications. The high-temperature stability, wide band gap, and established synthesis techniques of oxide materials make them highly attractive for a wide range of applications. These include industrial production (e.g., methane detection in mines) [2], the automotive industry (e.g., detection of pollutant gases from vehicles), medical applications (e.g., electronic noses mimicking the human olfactory system), indoor air quality monitoring (e.g., carbon monoxide detection), and environmental studies (e.g., greenhouse gas monitoring) [3].

The present work represents the first step toward developing a novel gas sensor from a thin film of copper oxide (CuO), as it has good energy gap properties for detecting certain gases. It is a typical semiconductor and possesses many outstanding properties, including catalytic activity, photoelectric properties, high stability, accessibility, and antibacterial activity. The results showed that CuO is stable under exposure to various gases and exhibits relatively low changes in base resistance. It is a less expensive technology than rare materials used in gas sensing applications [4]. Nanostructured thin films are distinguished by their stability, purity, strong adhesion to substrates, and low cost, making them suitable for a variety of applications. Deposition techniques for thin films have evolved significantly since the 1960s.

The emergence of advanced methods including DC magnetron sputtering offers high deposition rates, high film purity, and the capability to produce precise nanostructured layers. [1] The research gap addressed in this work lies in the need to enhance the performance of gas sensors based on CuO thin films, especially for ammonia detection, ensuring high, rapid, and stable responses at lower operating temperatures. In this study, copper oxide (CuO) thin films were fabricated on glass substrates using DC magnetron sputtering, investigate their structural, optical, and electrical properties, and to identify the phases obtained. These films were further employed as gas sensors to evaluate their efficiency in detecting ammonia (NH_3), while analyzing the influence of gas mixture ratios and thermal treatment conditions on sensing performance. The ability to tune the electrical and optical properties of these films by adjusting deposition parameters and thermal processing

is key to developing more effective nanostructured sensors. This research aims to bridge this gap by fabricating optimized nanostructured copper oxide films and systematically evaluating their physical, chemical, and electrical properties for efficient gas sensing applications [1 ,2, 3,4,5,6,7].

2. Materials and Methods

Figure (1) represents the gas inlet and flow control unit, which consists of two bottles of argon and oxygen gas. The two gases are connected by a gas mixer to produce the desired mixture. The pressure flow of the mixed gas into the plasma chamber is controlled by a needle valve (0-160 cm ^{3}). High-purity copper (Cu) targets (99.99%, Kurt J. Lesker, USA) were utilized for the deposition of copper oxide (CuO) thin films. The films were fabricated using a custom-designed DC magnetron sputtering system developed specifically for this study. The sputtering chamber was equipped with a rotary pump and a turbomolecular pump to achieve a base pressure of 3×10^{-5} mbar prior to deposition. High-purity argon (Ar, 99.999%) served as the sputtering gas, while high-purity oxygen (O_2, 99.999%) was introduced to regulate the oxidation process. glass substrates were ultrasonically cleaned sequentially in acetone, ethanol, and deionized water for 10 minutes each, followed by drying in a nitrogen stream. The deposition was carried out at a target-to-substrate distance of 2.5 cm, with controlled Ar:O_2 gas flow ratios of 1:1 and 2:1 using mass flow controllers. The DC sputtering power was maintained at 100 W, and the deposition time was optimized to achieve uniform film thickness. The structural properties of the films were analyzed using X-ray diffraction (XRD, PANalytical X'Pert PRO) with Cu Kα radiation (λ = 1.5406 Å). Surface morphology was examined using field-emission scanning electron microscopy (FE-SEM, JEOL JSM-7600F). The gas sensing performance toward NH_3 was tested in a custom-built sensing chamber by monitoring changes in electrical resistance at room temperature under various NH_3 concentrations.

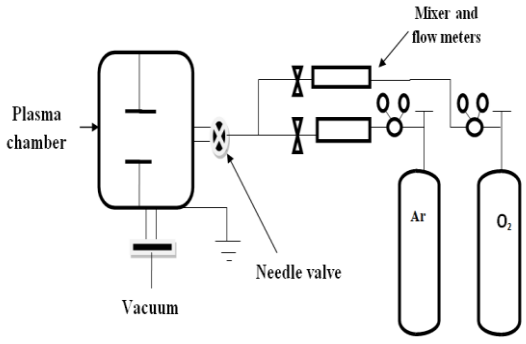

Figure 1: Schematic diagram of the gas inlet unit of the system.

3. Results and Discussion

1- XRD analysis

The crystal structure of the prepared CuO films was analyzed using X-ray diffraction (XRD) as shown in Figure (2). The patterns indicate that the films exhibit a monoclinic phase with a characteristic peak at $2\theta = 38.19^{o}$ for the sample with Ar:O_2 ratio 1:1 and $2\theta = 38.58^{o}$ for the 2:1 sample, corresponding to the (111) crystal plane according to JCPDS card no. 5-661 [8][9]. This confirms the formation of the nanostructured CuO films due to the bonding between copper and oxygen atoms during deposition with an average crystallite size of 34.77 nm for the 1:1 sample and 44.18 nm for the 2:1 sample [8].

These results demonstrated the molecular bonding between dispersed copper atoms and oxygen atoms to form copper oxide molecules and then deposit them on the underlying substrate.

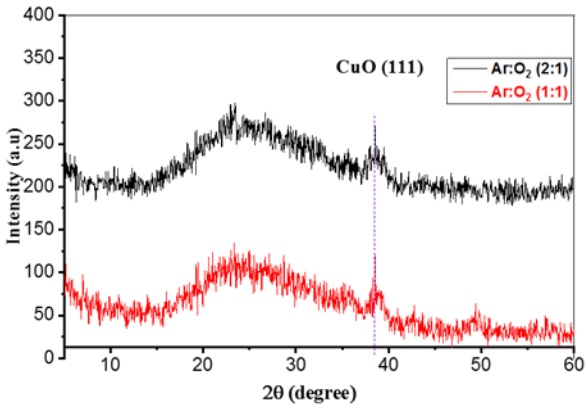

Figure 2: XRD diagram of CuO films with mixing (1:1)-(1:2).

2- a Field Emission Scanning Electron Microscope FE-SEM analysis

To evaluate the morphology of the composite nanoparticles, a Field Emission Scanning Electron Microscope (FESEM) was used at magnifications of 135k×, 70k×, 35k×, and 3k×. FESEM images of the prepared thin films deposited on glass substrates using the magnetron sputtering technique revealed that the particles grew in a nearly uniform and spherical-like shape as shown in Figure (3). The micrographs of the nanostructures of the CuO sample, which was prepared using a gas mixture of Ar:O_2 in a ratio of (1:1) at an electrode spacing of 2.5 cm without thermal treatment, indicated an average particle size of approximately 34.77 nm Figure (5) presents the micrographs of the nanostructures of the CuO sample, prepared using an Ar:O_2 gas mixture ratio of (1:2) at

the same electrode spacing (2.5 cm) without thermal treatment it showed an average particle size of about 44.18 nm.The results demonstrated that varying the Ar:O_2 mixing ratios can be effectively utilized to control several surface properties such as roughness and the particle size of CuO nanostructures, making them suitable for various applications.

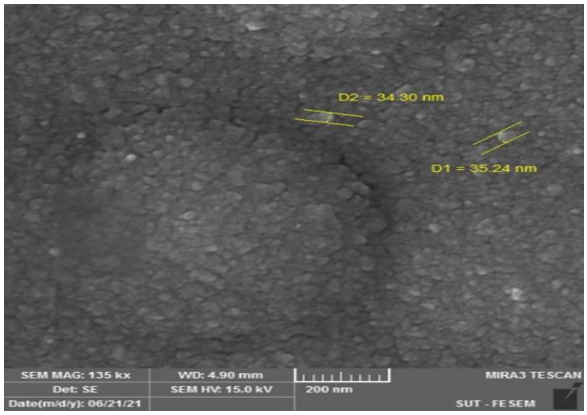

Figure 3: FESEM microscopic images of CuO nanostructures prepared using a mixture of Ar:O_2 gases of 1:1 at 2.5 cm distances between electrodes illustrating grain size measurements of approximately 34-35 nm.

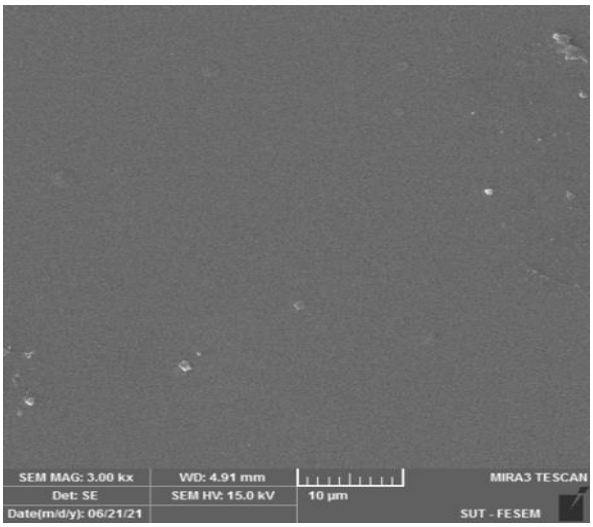

Figure 4: FESEM microscopic images of CuO nanostructures prepared using a mixture of Ar:O2 gases of 1:1 at low magnification (3k×), showing the film uniformity and surface coverage.

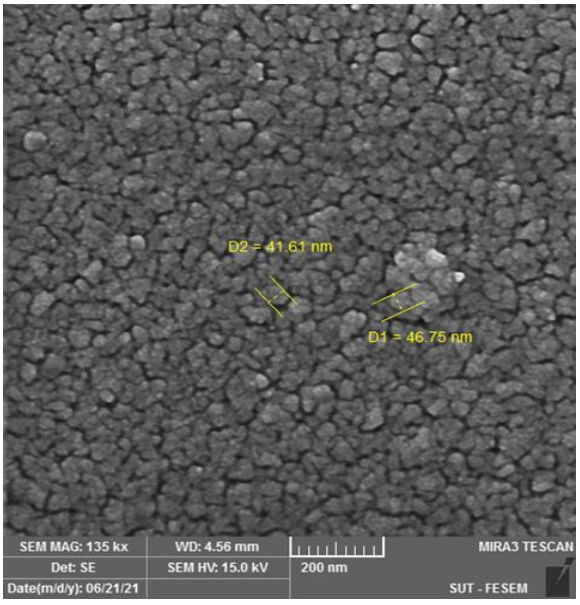

Figure 5: FESEM microscopic images of CuO nanostructures prepared using a mixture of Ar:O_2 gases of 1:2 at 2.5 cm between electrodes illustrating grain size measurements of approximately 41-47 nm.

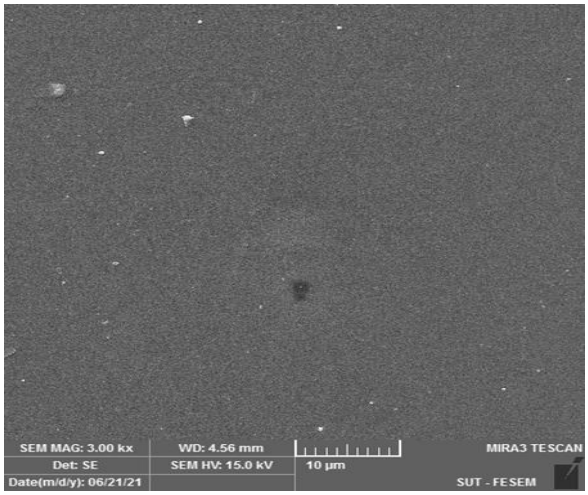

Figure 6: FESEM microscopic images of CuO nanostructures prepared using a mixture of Ar:O_2 gases of 1:2 at low magnification (3k×), showing the surface uniformity and coverage.

3-FourierTransformInfrared Spectroscopy FT-IR anylisis

Fourier-transform infrared spectroscopy (FT-IR) was employed in the wavenumber range of 400–4000 cm^{-1} to investigate the chemical bonds in CuO thin films, as shown in Figure (7,8). The spectra revealed characteristic Cu–O bonds corresponding to monoclinic CuO within the wavenumber range of 408.81–918.59 cm^{-1}, along with other chemical bonds summarized in Table (1).

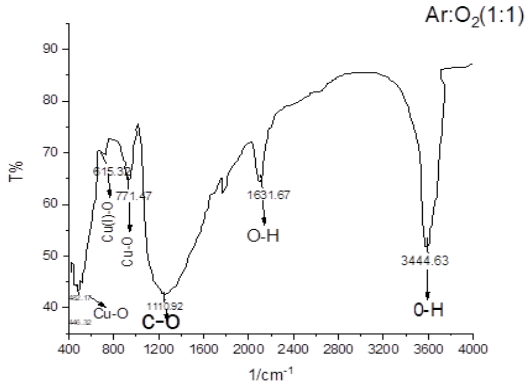

Figure 7: FTIR of CuO films with mixing ratio of (1:1).

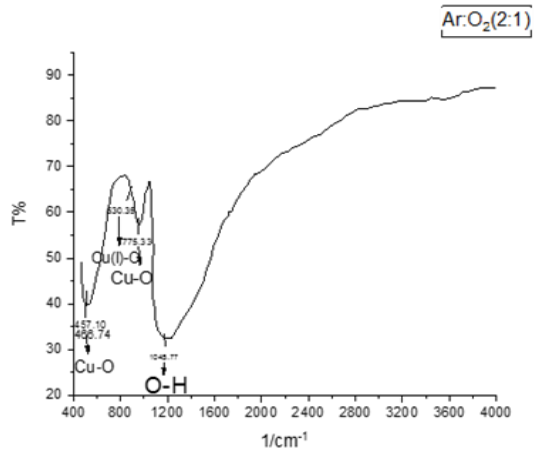

Figure 8: FTIR of CuO films with mixing ratio of (2:1).

Table 1: FTIR of CuO films at Ar:O_2 gas mixing ratios(1:1)-(1:2) where A mean Assignments,V.M Vibration Mode.

sample	Peak of FTIR $(cm)^{-1}$	Phase	A.V. M	[Ref.]
1:1	418.52,445.53 ,474.46 617.18 1643.24 1110.92 1643.24 2926.81 3400.10	CuO CuO CuO CuO CuO CuO Hydroxyls of absorbed water	Cu-O Cu-O C=O C-O C-O C-C Stretching vibration of O-H	[14] [14] [15] [15] [16] [17] [18]
1:2	408.81, 435.93 466.75,497.60 765.92,770.07 , 918.59 1047.33 1654.17 2341.58, 2376.71 3438.41 3454.27, 3756.43	CuO CuO CuO Cu(OH) CuO CuO Hydroxyls of absorbed water Hydroxyls of absorbed water	Cu-O Cu-O Cu-O Cu-OH C-C C-H Stretching vibration of O-H Stretching vibration of O-H	[19] [19] 20][18] [[21] [22] [23] [24] 26][26] [

4. Optical characteristics of (CuO) nano composites

The transmittance spectrum of copper oxide (CuO) films prepared by the magnetron sputtering method was obtained at a distance of 2.5 cm between electrodes with a time of 10 min and a gas mixing ratio of Ar:O2 (1:1, 2:2) within the wavelength range of 300-800 nm of the electromagnetic spectra using a UV-Spectrophotometer. The transmittance and absorption spectrum were also obtained, and the energy gap for direct electronic transitions was calculated.

4.1 **Transmittance (T)**

Figure nine illustrates the transmittance of CuO films prepared with a gas mixing ratio of Ar:O_2 (1:1) at an electrode distance of 2.5 cm, as a function of wavelength within the visible and near-infrared regions. It was observed that the transmittance of these films gradually increases with increasing wavelength in both regions. This increase can be attributed to the formation of new localized energy levels below the conduction band, which are capable of receiving electrons [10]. The same figure also shows the transmittance as a function of wavelength for the CuO film but with a gas mixing ratio of Ar:O_2 (2:1). In this case, the transmittance also increases gradually with wavelength and then tends to saturate[10]. However, which is lower than the previous one when the gas mixing ratio was 1:1, so the change in gases influences the permeability. This behavior is attributed to the quantitative size effect of the nanostructures [10].

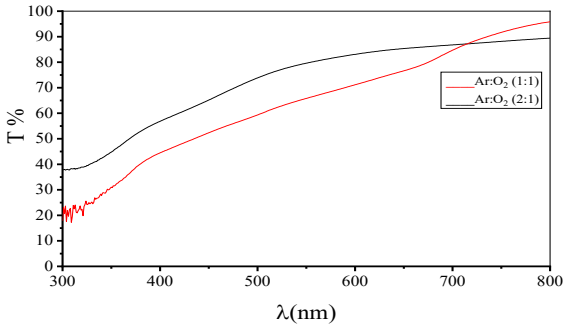

Figure 9: Transmittance as a function of wavelength for CuO fibers prepared by magnetron sputtering methods for (2.5 cm) between electrodes at Ar:O_2 gas mixing ratios.

4-2 Absorption Spectrum

Figure (10) shows the absorption spectrum as a function of wavelength for samples prepared at a distance of 2.5 cm and a mixing ratio of Ar:O2 gas (1:1, 1:2), respectively. It is observed that the absorption spectrum gradually decreases with increasing wavelength, which is unlike the transmittance spectrum. The absorption peak is likely related to the electronic transition that occurs from the valence band to the conduction band due to the particle's size [11]. The UV-visible absorption spectrum of CuO thin films is recorded in the wavelength region of 300-900 nm. It exhibits an intense peak centered at ~320 nm, which is attributed to the dispersive nature of the size variation of the nanoparticles. Within the infrared region, it has been shown that the absorption spectrum has a large value at short wavelengths and gradually decreases with increasing wavelength for all prepared films, as the energy in this region of the spectrum is less than the energy gap of the semiconductor material;therefore, this photon does not transfer electron its energy does when absorbing it .

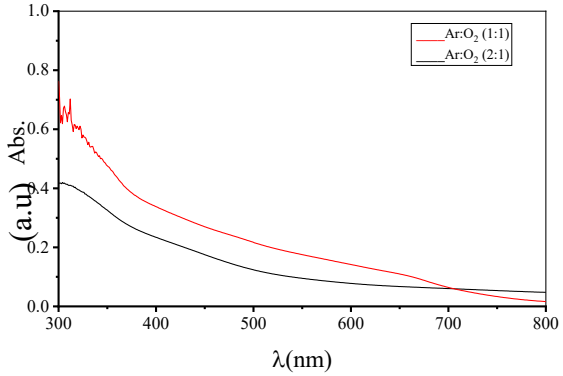

Figure 11: Absorbance as a function of wavelength for CuO films prepared by magnetron sputtering at a distance of (2.5 cm) between electrodes at Ar:O2 gas mixing ratios.

4-3 Optical energy gap (E_g)

Figure (11) shows the transmittance and reflectance spectra of distinct copper oxides formed under varying total pressures. Tauc's relationship can be used to determine the values of Eg from the transmittance and reflectance: [7 ,12,13]

$(\alpha h\nu)^n = A(h\nu - E_g)$ ….. (1)

where hν denotes the incident photon energy and A denotes the material constant. The

measured values of n are (2, 1/2, 3, and 3/2), respectively, corresponding to the allowed direct, allowed indirect, forbidden direct, and forbidden indirect transitions. The indirect band gap of CuO can be taken into account, and thus n = 1/2. [2, 26]. The absorption coefficient α t is the percentage of decrease in the flux of incident radiation energy per unit distance in the direction of wave propagation within the medium. The absorption coefficient depends on the photon energy (hv) and on the properties of the semiconductor in terms of the type of electronic transitions and its energy gap. can be calculated using the following formula:

$$\alpha = 1/d \ln[(1-R)^2/T] \quad ..(2)$$

Where d is the film thickness, and R and T are the reflectance and transmittance, respectively. Figure (7) shows the photon energy dependence of $(\alpha hv)^n$ values. The optical energy gap (E_g) can be defined as the minimum energy required to transfer an electron from the valence band to the conduction band. From Figure (12), the calculated optical Eg values are found to be CuO 2.33 at mixing ratio 2:1 and 2.21 eV mixing ratio 1:1. These results are consistent with those in previous studies W. Zheng [27, 28]. Furthermore, despite the fluctuations in the morphology of the films under different O_2 partial pressures, the band gap value for each type of single-phase copper oxide remains approximately constant, in accordance with the observed band gap results. This means that the Cu2O/CuO ratio in the mixed phase can be adjusted to modify the band gap of the copper oxide films[19].

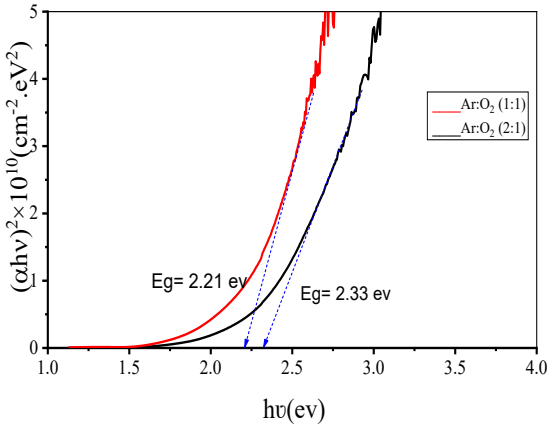

Figure 12: The allowed direct optical energy gap of CuO films whith mixing ratios(1:1) – (1:2).

5- Sensitivity for Gases (NH_3)

Table two and figure ten shows that the highest sensitivity of the CuO sensor to NH3 gas is 13.62% at an operating temperature of 200 K and then begins to decrease with the decrease in the mixing ratio. When comparing the results of the tables, we find that the sensitivity of the membranes to the gas decreased with the increase in the operating temperature. We conclude that the prepared CuO membrane has the highest sensitivity value of 13.62%. This is due to the

fact that the absorption of adsorbed molecules increases rapidly when the conditions change, which reduces the presence of ammonia on the surface, thus reducing the response [29]. This confirms that it is a good sensor for detecting NH3 gas. The higher sensitivity can also be attributed to the optimal surface roughness, porosity, large surface area and large oxidation rate.. In order to determine the sensitivity parameters, primarily the response time and recovery time of the artificial CuO gas sensor detector, a suitable setup is made. Using a gas sensor test system, which is a homemade device, the gas sensitivity can be defined as the percentage change in the sensor's conductivity when exposed to the target gas compared to the sensor's conductivity in air. This leads to the following equation: [29]

$$S\% = \frac{G_g - G_a}{G_a} \times 100\ \% \quad \dots\ (\ 3\ )$$

where Ga: the sensor's conductivity in air, and Gg: the conductivity in the presence of the target gas [30]. In this study, it was found that the change in electrical conductivity of the manufactured CuO samples with operating temperature, as the operating temperature is one of the most important factors affecting the responses of oxide sensors, and the operating temperature for copper oxide is (30, 100, 200, 300) C°. In the presence of NH_3 gas, the maximum value of the sensors for CuO. gas sensitivity (S_g) was 16.6 for NH_3 gas at 200 °C. Figure (10) represents the relationship between sensitivity and operating temperature for NH_3gas.

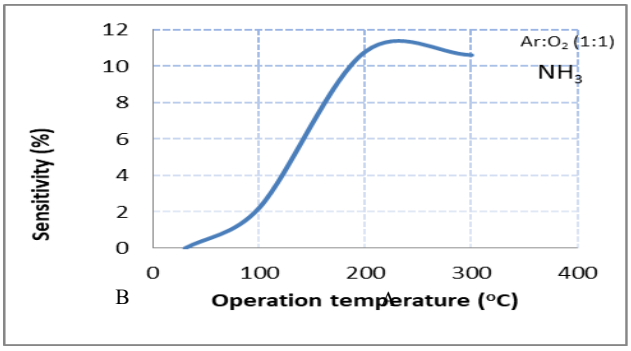

Figure 13: Sensor sensitivity as a function of operating temperature for CuO for filims (1:1) mixing ratios, in the presence of NH_3 gas.

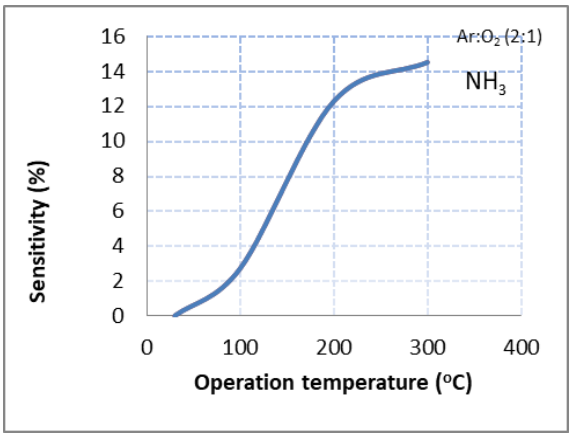

Figure 14: Sensor sensitivity as a function of operating temperature for CuO for filims (1:2) mixing ratios, in the presence of NH_3 gas.

Table 2: Values of optimum sensitivity, response and recovery times, and operating temperature for CuO samples Ar:O_2 mixing ratios, which were evaluated for NH_3 gas sensing performance.

NH_3				
Sample	Operating Temp.	Sensitivity (%)	Response time (s)	Recover time (s)
CuO (1:1)	200 °C	10.8	27	51.3
CuO (2:1)	200 °C	14.62	26.1	51.3

5-Results of Sensitivity for Gase NH_3

5-1Response and Recovery Times

The response time is defined as the time required for the sensor's resistance to reach 90% of its final value when exposed to the target gas. The recovery time is defined as the time required for the resistance to decrease to 10% of its original value when the sensor is returned to fresh air. Figure (11) shows the response and recovery time values for samples prepared from CuO films. It was found that the CuO films exhibit semiconductor behavior at operating temperatures exceeding 200 °C. An increase in the response was observed with increasing temperature, while the highest sensitivity was recorded at 200 °C. Then, the values decreased at higher temperatures, which was attributed to the regular increase in the electrical conductivity of the prepared samples.

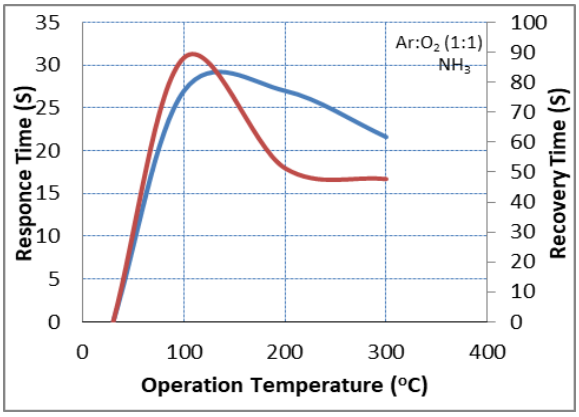

Figure 15: Response time and recovery time of CuO films at Ar:O2 mixing ratios(1:1) for NH_3 gas.

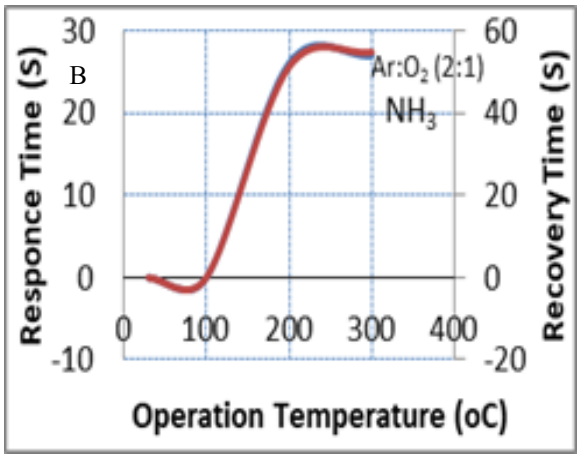

Figure 16: Response time and recovery time of CuO films at Ar:O2 mixing ratios(1:2) for NH_3 gas.

4. Conclusion

High-quality copper oxide nanoparticles can be prepared using DC magnetron spatring technology. The difference in argon and oxygen gases in the discharge plasma is a key

factor in the effective harvesting of the prepared nanoparticles, particularly surface roughness and wind density. This reliable technique yields nanostructures of copper components in both phases, which can be exploited in technical applications, especially in the field of gas sensors. The prepared nanostructures also showed significant improvement when tested as gas detectors, confirming their efficiency and reliability in such vital applications.

5. References

1. Franklin A. D., (2015). DEVICE TECHNOLOGY. Nanomaterials in transistors: From high-performance to thin-film applications. Science (New York, N.Y.). 349, 6249, aab2750.
2. Dolai S., Dey R., Das S., Hussain S., Bhar R., and Pal A. K., (2017). Cupric oxide (CuO) thin films prepared by reactive dc magnetron sputtering technique for photovoltaic application. Journal of Alloys and Compounds. 724, 456-464.
3. Soni N., and Nigam N., (2025). Recent Advances in Artificial Intelligence and Machine Learning: Trends, Challenges, and Future Directions. International Journal of Engineering Trends and Applications (IJETA). 12, 1, 9-12.
4. Muratore C., Moore J. J., and Rees J. A., (2003). Electrostatic quadrupole plasma mass spectrometer and Langmuir probe measurements of mid-frequency pulsed DC magnetron discharges. Surface and Coatings Technology. 163, 12-18.
5. Chen F. F., (2001). Langmuir probe analysis for high density plasmas. Physics of Plasmas. 8, 6, 3029-3041.
6. Patil G. E., Kajale D. D., Chavan D. N., Pawar N. K., Ahire P. T., Shinde S. D., and Jain G. H., (2011). Synthesis, characterization and gas sensing performance of SnO_2 thin films prepared by spray pyrolysis. Bulletin of Materials Science. 34, 1, 1-9.
7. Chen C. H., Kelder E. M., and Schoonman J., (1996). Unique porous $LiCoO_2$ thin layers prepared by electrostatic spray deposition. Journal of materials science. 31, 20, 5437-5442.
8. Pan J., Yang C., and Gao Y., (2016). Investigations of Cuprous Oxide and Cupric Oxide Thin Films by Controlling the Deposition Atmosphere in the Reactive Sputtering Method. Sensors and Materials. 28, 7.
9. Khadyair A. A., Wanas A. H., and Zije B. A., (2018). Study the Structural and Optical Properties of CuO Thin films Prepared by dc Magnetron Sputtering. Journal of Kufa-Physics. 10, 2, 61-67.

10. Stenzel O., (2005). The physics of thin film optical spectra: an introduction. Berlin, Heidelberg: Springer Berlin Heidelberg.
11. Yin M., Wu C. K., Lou Y., Burda C., Koberstein J. T., Zhu Y., and O'Brien S., (2005). Copper oxide nanocrystals. Journal of the American Chemical Society. 127, 26, 9506-9511.
12. Miguel A. M. Palazon., (2000). Carbon nitride deposition by magnetron sputtering: Structural, mechanical, electrical and optical properties (PhD thesis). Dublin City University, Ireland.
13. Dolai S., Das S., Hussain S., Bhar R., and Pal A. K., (2017). Cuprous oxide (Cu_2O) thin films prepared by reactive d.c. sputtering technique. Vacuum. 141, 296-306.
14. Zou G., Li H., Zhang D., Xiong K., Dong C., and Qian Y., (2006). Well-aligned arrays of CuO nanoplatelets. The Journal of Physical Chemistry B. 110, 4, 1632-1637.
15. Uhlrich J. J., Yang B., and Shaikhutdinov S., (2014). Methanol reactivity on silica-supported ceria nanoparticles. Topics in Catalysis, 57, 14, 1229-1235.
16. Rahim S., Sasani G. M., and Radiman S., (2012). Surface modification of titanium oxide nanocrystals with PEG. Scientific Iran. 19, 3, 948-953.
17. Bhosale M. A., and Bhanage B. M., (2016). A simple approach for sonochemical synthesis of Cu_2O nanoparticles with high catalytic properties. Advanced Powder Technology. 27, 1, 238-244.
18. Gaewdang T., and Wongcharoen N., (2017). Influence of oxygen flow rate on structural, optical and electrical properties of copper oxide thin films prepared by reactive magnetron sputtering. IOP Conference Series: Materials Science and Engineering, 211, 1, 4-9.
19. Kliche G., and Popovic Z. V., (1990). Far-infrared spectroscopic investigations on CuO. Physical review B. 42, 16, 10060.
20. Betancourt-Galindo R., Reyes-Rodriguez P. Y., Puente-Urbina B. A., Avila-Orta C. A., Rodríguez-Fernández O. S., Cadenas-Pliego G., and García-Cerda L. A., (2014). Synthesis of copper nanoparticles by thermal decomposition and their antimicrobial properties. Journal of Nanomaterials. 2014, 1, 980545.
21. Fterich M., Ben Nasr F., Lefi R., Toumi M., and Guermazi S., (2016). Effect of concentration of hexamethylene tetramine in structure, microstructure and optical properties of CuO nanoparticles synthesized by hydrothermal route.

Materials Science in Semiconductor. 43, 114-122.

22. Bhuvaneshwari V., Vaidehi D., and Logpriya S., (2018). Green synthesis of copper oxide nanoparticles for biological applications. Microbiol Curr Res. 2, 1, 9-10.
23. Sundaramurthy N., and Parthiban C., (2015). Biosynthesis of copper oxide nanoparticles using Pyrus pyrifolia leaf extract and evaluation of catalytic activity. International Research Journal of Engineering and Technology (IRJET). 2, 6, 332-338.
24. Guo D., Wang L., Du Y., Ma Z., and Shen L., (2015). Preparation of octahedral Cu_2O nanoparticles by a green route. Materials Letters. 160, 541-543.
25. Singh P. K., Kumar P., Hussain M., Das A. K., and Nayak G. C., (2016). Synthesis and characterization of CuO nanoparticles using strong base electrolyte through electrochemical discharge process. Bulletin of Materials Science. 39, 2, 469-478.
26. El-Trass A., Elshamy H., El-Mehasseb I., and El-Kemary M., (2012). CuO nanoparticles: Synthesis, characterization, optical properties and interaction with amino acids. Applied. 258, 7, 2997-3001.
27. Zheng W., Chen Y., Peng X., Zhong K., Lin Y., and Huang Z., (2018). The phase evolution and physical properties of binary copper oxide thin films prepared by reactive magnetron sputtering. Materials. 11, 7, 1253.
28. Alajlani Y., Placido F., Barlow A., Chu H. O., Song S., Rahman S. U., and Gibson D., (2017). Characterisation of Cu_2O, Cu_4O_3, and CuO mixed phase thin films produced by microwave-activated reactive sputtering. Vacuum. 144, 217-228.
29. Jabber A. A., and Abdulridha A. R., (2025). Preparation and characterization of CuO/ZnO nanostructures thin films using thermal evaporation for advanced gas sensing applications. Trends in Sciences. 22, 3, 9002-9002.
30. Suresh S., (2014). Studies on the dielectric properties of CdS nanoparticles. Appl Nano. 4, 3, 325-329.